AIAA JOURNAL
Vol. 32, No. 2, February 1994

Parametric Computational Study of Isolated Blade-Vortex Interaction Noise

Judith M. Gallman*
NASA Ames Research Center, Moffett Field, California 94035

A parametric study was performed to quantitatively describe how the vortex core size, the vortex location, and the hover-tip Mach number M_h affect blade-vortex interaction (BVI) noise. The effects of these parameters on BVI noise are determined using a rotor acoustic prediction program. The acoustic prediction program is based on the well-known Ffowcs Williams and Hawkings equation for acoustic pressure, wherein noncompact monopole terms model rotor blade thickness and distributed dipoles model local blade surface pressure. The dipole strengths are determined by an unsteady, three-dimensional, full-potential rotor code that models the aerodynamic interactions between a nonlifting rotor and a tip vortex generated by an upstream wing. The acoustic pressures were calculated for several observer positions in regions of intense acoustic radiation for a variety of blade-vortex proximities, orientations, hover-tip Mach numbers, and vortex-core sizes. This study has quantified the sensitivity of BVI noise to the dominant vortex and aerodynamic parameters. The sound pressure level (SPL) falls off as the inverse of the square of the miss distance between the vortex core and the rotor blade when the miss distance is greater than the core radius. Increasing the core radius is not as effective as increasing the miss distance when attempting to reduce BVI noise. As expected, this study shows that SPL decreases with an increase in the obliqueness of interaction. The calculations performed in this work indicate that SPL increases approximately as M_h^8. These results can be used to guide future research of BVI noise reduction.

Nomenclature

a = vortex core radius
a_0 = speed of sound in air
C_G = chord of the vortex generator
c = chord
d = distance from the rotor hub to the observer
M_h = hover-tip Mach number
M_r = Mach number in the radiation direction
p' = acoustic pressure
R = rotor blade radius
r = radial distance from the center of rotation
$\hat{r}_i$ = unit vector describing the acoustic radiation direction
t = observer time
U = rotor speed
U_s = simplified rotor speed
V = total velocity
V_i = local freestream velocity vector
$V_{\max}$ = maximum tangential vortex velocity
V_q = vortex velocity
$V|_a$ = vortex velocity for $r = a$
V_∞ = freestream velocity, tunnel speed
x = observer location
x/c = distance of the vortex generator from the rotor centerline
z/c = miss distance, distance between vortex center and blade mean chord
α = longitudinal angle between the observer plane and the plane of the rotor hub (see Fig. 6)
β = lateral angle between the observer plane and the direction of flight (see Fig. 6)
Γ = vortex strength, circulation
μ = advance ratio
ρ = density
τ = retarded time, source time
ϕ = velocity potential
Ψ = rotor azimuth angle
Ω = rotor rotational speed

Received May 5, 1992; presented as Paper 92-02-119 at the DGLR/AIAA 14th Aeroacoustics Conference, Aachen, Germany, May 12–15, 1992; revision received May 27, 1993; accepted for publication May 28, 1993. This paper is declared a work of the U.S. Government and is not subject to copyright protection in the United States.

*Research Scientist, Fluid Mechanics Division, U.S. Army Aeroflightdynamics Directorate, ATCOM, Mail Stop 215-1. Member AIAA.

Introduction

In powered descent, a helicopter's tip vortices interact with its main rotor blades. These interactions result in sudden changes in blade loading which contribute substantially to high noise and vibration levels. The induced velocity associated with a tip vortex is the predominate parameter that governs noise produced by blade-vortex interactions (BVI).[1] The magnitude of the induced velocity is governed by the proximity of the vortex to the blade and the properties of the vortex, such as strength and core size. To reduce the noise levels, the velocities induced on the rotor blade must be decreased. Possible approaches are to reduce the vortex strength, increase the distance between the blade and the vortex, or increase the size of the vortex core. It is difficult to reduce the vortex strength without a performance penalty (unless the number of blades is increased) since the vortex strength is directly related to the blade lift. Recent experiments in higher harmonic control of the blade pitch angle have studied the reduction in noise by changing the miss distance between the rotor blade and the vortex. However, in these experiments, the miss distance could not be measured easily, and the reduction in noise was referenced to the higher harmonic input.[2,3] Past experiments have attempted to increase the core size by varying the blade tip geometry. The most successful of these attempts has been the ogee tip where the radiated noise was decreased without a performance penalty.[4,5] However, the correlation between the increase in core size and the reduction in noise has not been quantified. The goal of the parametric study in the current work is to quantify the effect of miss distance, core size, hover-tip Mach number, and obliqueness of interaction on BVI noise and thereby determine the influence of the vortical velocities.

Widnall and Wolf[6] studied the effects of tip-vortex structure on BVI noise. In their study, they represented the unsteady upwash induced on the airfoil as a distribution of sinusoidal gusts that cause a sinusoidal variation in lift along the rotor span. Incompressible theory was used to calculate the unsteady spanwise lift distribution. A solution to the acoustic

wave equation was determined by prescribing the unsteady lift distribution as the boundary condition on the blade. This analysis was applied to blade vortices shed by elliptical-, linear-, and cosine-squared blade loading distributions. Widnall and Wolf's study has shown that the BVI noise is quite sensitive to changes in the vortex structure when the miss distance is less than half the blade chord.

The direct influence of the vortical velocities on BVI noise is studied in the current work with the combination of a full-potential rotor code (FPR)[7] and a rotor acoustic prediction program (RAPP).[8] Tadghighi et al.[9] also combined a full-potential computational fluid dynamics (CFD) code (RFS2) with an acoustic code (WOPWOP) to predict BVI noise. In their work, a wake geometry was determined that would yield good correlation with experimental data. The quality of the correlation was extremely dependent on the comprehensive analytic model of rotor aerodynamics and dynamics (CAMRAD)-predicted geometry of the interacting vortex elements and the orientation of these elements with respect to the blade. Their results indicated that CAMRAD's free wake model, used to predict the tip-vortex trajectories, produces "lower streamwise and higher axial wake convective velocities than those inferred from experimental data."[10] To eliminate the need for a wake analysis, the parametric study in the current work models a vortex generator that is upstream of a nonlifting rotor. The rotor interacts with, but does not generate, the vortex (see Fig. 1). This type of interaction is known as an isolated rotor-vortex interaction and is ideal for a quantitative analysis of BVI noise since all of the vortex properties—strength, core size, and location—are prescribed.

The pressure change caused by the interaction of the nonlifting blade with the externally generated vortex is similar in nature to the pressure change caused by the interaction of a rotor with its own shed vortex. This was shown experimentally in Ref. 11. The comparisons of measured leading-edge pressure, shown in Fig. 2, are from the experiment of Ref. 11 and illustrate that the isolated rotor-vortex interaction captures the physics of the self-generated, parallel, blade-vortex interaction quite well. The smaller pressure jump and shorter characteristic time for the pressure rise of the self-generated vortex are attributed to differences in vortex proximity and core size.

Predicted airloads from the full-potential code have compared well with experimental data for isolated rotor-vortex interactions,[12] and the results from the acoustic prediction code have compared well to experimental data for BVI flight

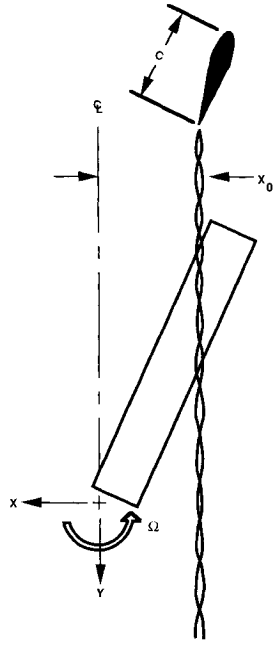

Fig. 1 Schematic of the isolated blade-vortex configuration.

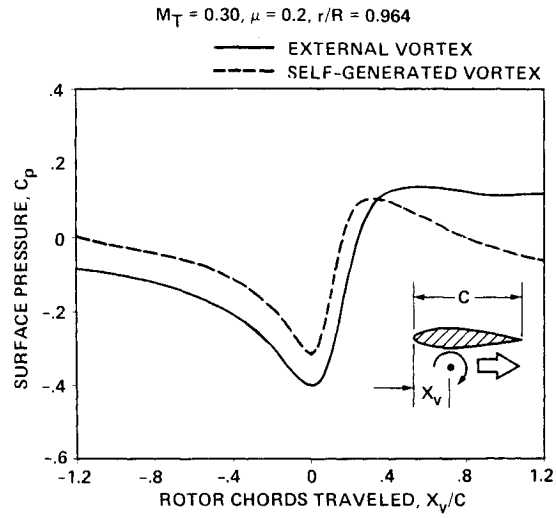

Fig. 2 Comparison of measured leading-edge pressures for parallel BVIs with external and self-generated vortices.[11]

regimes when the experimentally measured blade loading was used as input.[8] This suggests that the combined CFD/acoustic-prediction code would yield fairly accurate acoustic results for the isolated BVI. The pertinent details of the computer models used for the parametric study are described in the following sections of this paper.

Computational Methods

Full-Potential Rotor Code

The full-potential rotor (FPR) code solves the three-dimensional, unsteady, full-potential equation for transonic flow with the density function determined by the Bernoulli equation. This rotor code, in strong conservation form, is based on the fixed-wing code of Bridgeman et al.[13] Discrete vortices are introduced into the finite difference computations using a velocity decomposition method. The total velocity field is the sum of the gradient of the potential and the known vortex velocity.

$$V = \nabla\phi + V_q \tag{1}$$

The potential equation takes the form

$$\rho_t + \nabla \cdot (\rho \nabla\phi) = \nabla \cdot \rho V_q \tag{2}$$

and is solved using half-point differencing formulas. First-order backward differencing is used in time and second-order differencing is used in space.[12,14] An exponential vortex model

$$V_q = \frac{\Gamma}{2\pi r}\left[1 - e^{-(r^2/a^2)}\right] \tag{3}$$

is used to determine the velocities associated with the vortex. This model assumes that all of the vorticity is confined to a central core which has a radius defined by $V|_a = V_{\max}$. The location of the vortex is defined by the distance below the tip-path plane and the distance from the centerline of the rotor system (see Fig. 1). The vortex velocity field is specified at grid points in the computational field, not just on the blade surface. This allows for more accurate predictions of the surface blade pressures.

The grids for the solution are a spanwise series of body-fitted O-grids with 80 points in the chordwise direction, 25 points in the spanwise direction, and 25 points in the normal direction. The time step for the solution corresponds to 0.125 deg rotor azimuth per time step, or about 64 time steps per chord at the rotor tip. The reason for this relatively small time step is to capture the BVI events that happen in a very short period of time.

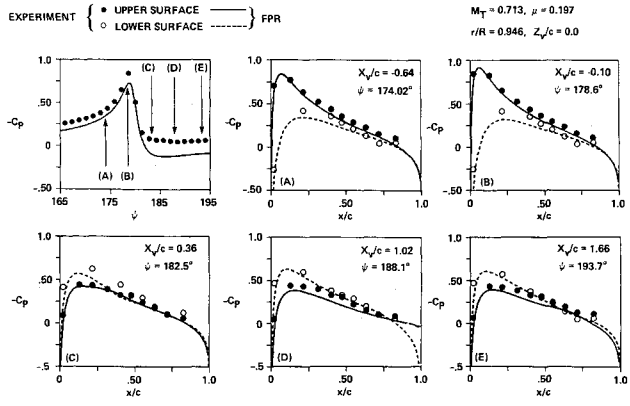

Fig. 3 Computational and experimental comparisons for a parallel BVI, $M_h = 0.713$, $\mu = 0.197$, $r/R = 0.946$, and $z/c = 0.0$.[12]

Figure 3 shows comparisons of computed and experimental blade surface pressures for a parallel rotor BVI. The experiment was performed by Caradonna et al.[11] and the computations, performed by Caradonna and Strawn,[12] are a simulation of this experiment using FPR. The good comparisons between the computed solutions and the measured data make it possible to confidently perform the parametric study proposed in the current work. Note that the comparisons are for a miss distance equal to zero, $z/c = 0$. The comparisons indicate that, even though FPR does not explicitly model the vortex distortion that occurs in a direct hit, the split potential used in FPR does account for some changes imparted to the vortex during interaction.

Rotor Acoustic Prediction Program

A simple, yet accurate, rotor acoustic prediction program (RAPP) utilizes the Ffowcs Williams and Hawkings (FW-H) equation in a form well suited to incorporate blade surface pressure from computational codes such as FPR. The FW-H equation

$$4\pi p'(\boldsymbol{x}, t) = \frac{\partial}{\partial t}\int\left[\frac{\rho_0 v_n}{r|1-M_r|}\right]_{\text{ret}} \mathrm{d}S(y) + \frac{1}{a_0}\frac{\partial}{\partial t}\int\left[\frac{p_i \hat{r}_i}{r|1-M_r|}\right]_{\text{ret}} \mathrm{d}S(y) + \int\left[\frac{p_i \hat{r}_i}{r^2|1-M_r|}\right]_{\text{ret}} \mathrm{d}S(y) \tag{4}$$

is an integral representation of the inhomogeneous wave equation that is valid in all space and governs acoustic pressure generated by moving bodies. The inhomogeneous terms describe mass displacement due to bodies in motion and forces of local surface stresses, such as viscous and pressure stresses.[15] The subscript ret indicates that the integrals are to be evaluated at the retarded time $\tau = t - r/a_0$. The speed of propagation of sound in the fluid medium is designated by a_0, and ρ_0 is the density of the undisturbed fluid medium. M_r is the Mach number in the radiation direction, $M_r = V_i \hat{r}_i / a_0$, where V_i is the local freestream velocity vector, and $\hat{r}_i$ is the unit vector in the radiation direction.

The first term on the right-hand side of Eq. (4) is referred to as the thickness term. This term represents the disturbance of the fluid medium caused by the airfoil. The second and third terms are the loading terms. These terms represent the noise caused by the airfoil exerting a force on the fluid. Equation (4) does not contain the Lighthill stress tensor, and it is not included in the computation performed by RAPP. The Lighthill stress tensor is a volume integral that models the noise produced by high-speed flow. It is assumed in the current work that the blade-vortex interactions do not result in strong shocks and that the contribution to noise from this high-speed flow term is negligible.

RAPP uses the acoustic lifting line method to model the blade surface loading. The acoustic lifting line is the quarter chord of the acoustic planform which consists of the locations of the contributing sources. These source locations are found by solving the retarded time equation $t = \tau + r(\tau)/a_0$, where t is the observer time, τ is the source time, and $r(\tau)$ is the distance between the source and the observer.[16]

In this formulation, the force terms in the FW-H equation are modeled as chordwise compact sources with five spanwise source locations along the quarter chord of the acoustic planform. Note that the term "acoustic lifting line" refers to the location of the contributing sources, not to the method of determining the aerodynamics. The aerodynamic sectional coefficients that describe the source strengths are calculated by FPR and contain information over the whole chord. This technique works well as long as there is sufficient azimuthal resolution of the sectional lift and drag input.

Figure 4 shows comparisons of measured and predicted acoustic pressure time histories. The measured data was acquired during the aerodynamic and acoustic testing of model rotors program at the Duits-Nederlands Windtunnel (DNW). The Boeing model 360 data are considered to be of high quality to validate acoustic prediction codes.[17] For the predictions shown in Fig. 4, blade surface pressure measurements provided the loading information. The sectional coefficients were calculated from the chordwise pressure distributions. All available information about the interaction is present in the coefficients. Even though the pressure measurement devices were distributed over three of the blades, they were applied in the acoustic calculations as if they were all acquired from the same blade. Therefore, the blade-to-blade differences present in the experimental acoustic data are not present in the computations. For the observer at $\alpha = 25$ deg and $\beta = 30$ deg, the blade-to-blade differences are quite drastic and the predicted signal does not closely resemble any one of the four signals, but does

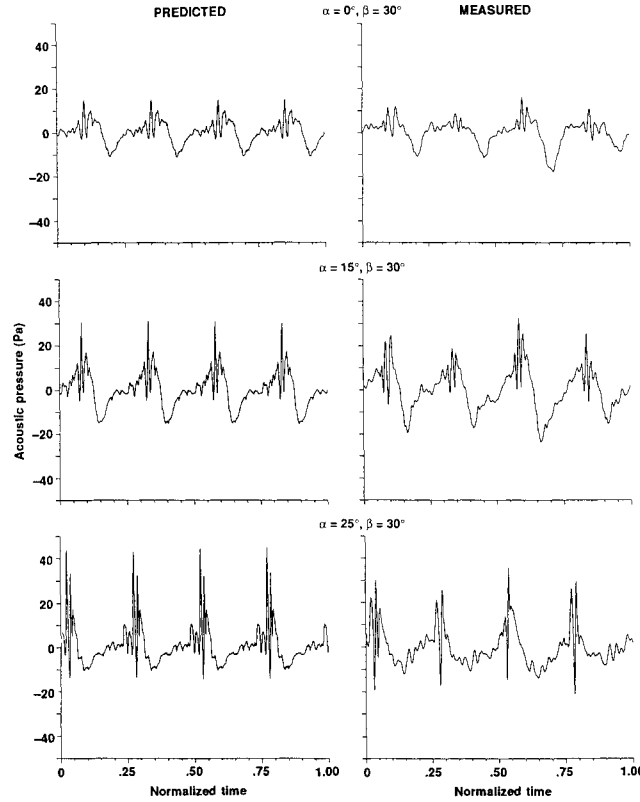

Fig. 4 Computational and experimental acoustic-pressure time histories with $M_h = 0.64$, $\mu = 0.225$, $C_T = 0.07$, and shaft tilt = 4.38 deg.

contain features from each. With this in mind, the comparisons in Fig. 4 indicate that the BVI noise can be predicted accurately when appropriate loading information is supplied to the acoustic prediction code. Therefore, the sectional lift and drag, supplied by FPR at 0.125-deg intervals about the azimuth at five radial stations, is used to predict the BVI noise in this parametric study.

FPR-RAPP Combination

To determine how well the FPR-RAPP prediction of the noise produced by an isolated BVI compares to the noise produced by a self-generated BVI, the predicted acoustic-pressure time history for a parallel, isolated BVI computed using the FPR-RAPP combination is compared to an experimentally measured, self-generated BVI. The experiment was conducted in the DNW with a 1/7 geometrically scaled AH-1/OLS model.[18] The two-bladed model has a rectangular tip, a rotor radius of 3.143 ft (0.958 m), and a chord of 0.34 ft (0.104 m). The airfoil is a modified AH-1S 540 airfoil and is 9.71% thick. The geometry for the model used in the FPR-RAPP prediction is discussed in the next section. The comparison in Fig. 5 shows the qualitative similarities between this study and the experiment. The two time histories are similar in shape with a negative peak followed by a larger positive peak. The second peak in the experimentally measured acoustic-pressure time history is caused by the blade interacting with a second vortex. There is only one interaction for the isolated BVI and therefore there is no second peak in the time history. The difference in phase between the two signals is due to the difference in interaction location and observer location. The isolated BVI occurs at 180-deg rotor azimuth, whereas the self-generated BVI occurs between 60- and 90-deg rotor azimuth. Although the vortex characteristics of the self-generated vortex (strength, core size, and miss distance) are unknown and a quantitative comparison is not possible, the similarity of the two time histories is encouraging.

Results

The change in sound pressure level (SPL) with miss distance, core size, rotor speed, and obliqueness of interaction calculated using the FPR-RAPP combination is a good measure of the sensitivity of BVI noise to these parameters, especially when one considers the ability of both FPR and RAPP to produce accurate predictions of rotor airloads and rotor acoustics, respectively. Also, the isolated vortex-blade interaction has been shown to be a good model of self-generated vortex-blade interaction.

This computational, parametric study was performed as if a vortex generator were upstream of a nonlifting rotor (see Fig. 1). The rotor blades are untwisted with rectangular

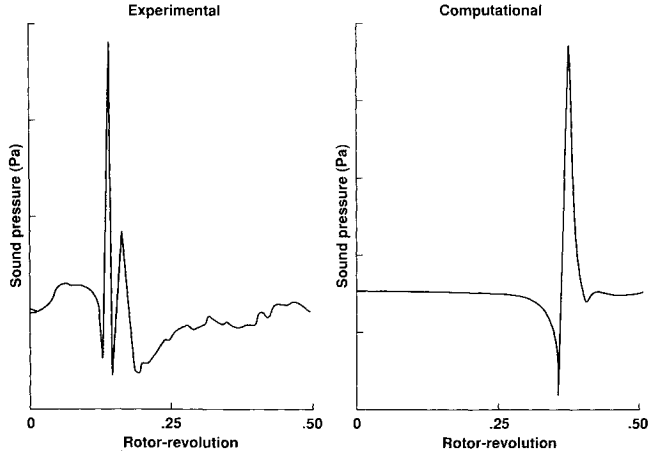

Fig. 5 Comparison of a predicted acoustic-pressure time history for an isolated, parallel BVI to an experimentally measured, acoustic-pressure time history for a self-generated, parallel BVI.

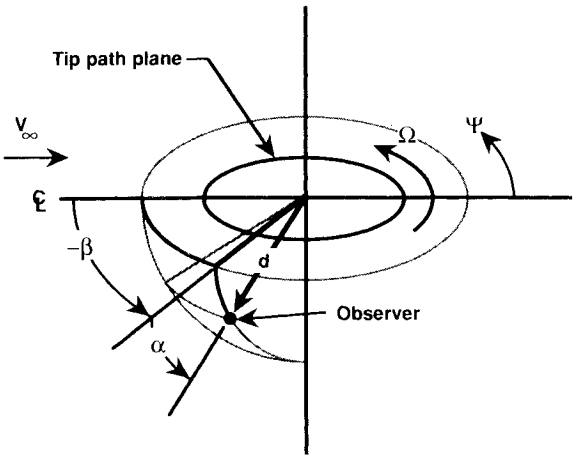

Fig. 6 Definition of observer location with α positive below the tip-path plane, and β positive to the right of the centerline (the angle shown above is negative).

tips, radii of 3.5625 ft (1.086 m), constant chord of 0.5 ft (0.1524 m), and NACA 0012 airfoil sections. The core radius and vortex strength used in this study are based on measurements made by McAlister and Takahashi[19] of tip-vortex structure produced by wing geometries similar to the vortex generator used in the experiment of Refs. 11 and 12.

The definition of the observer location is shown graphically in Fig. 6. The observer location is defined by d, the distance from the rotor hub; α, the angle below the tip path plane; and β, the angle from the direction of flight. For all observer locations in this study, $d = 3.44R$. This distance is assumed large enough to consider the observer in the "far field."

The SPLs shown in Figs. 7 and 9–11 contain only the noise caused by the interaction of the blade with the vortex. This is accomplished by including only the loading terms (the second and third terms) from Eq. (4) in the calculation. The thickness noise is not included because it does not contribute to the understanding of BVI noise. The SPLs are determined by performing a Fourier transform on one period of the calculated acoustic pressure time history. The Fourier coefficients are squared and summed to determine the root-mean-square pressure and the SPL (re 2×10^{-5} Pa).

Miss Distance

One approach to reducing BVI noise is to increase the distance between the vortex and the rotor blade. To study the effect of miss distance z/c on BVI noise, the miss distance was varied from 0 to 100% of the chord whereas all other parameters—advance ratio $\mu = 0.197$, hover-tip Mach number $M_h = 0.713$, vortex strength $\Gamma = -0.17a_0c$, and core radius $a = 0.17c$—were held constant. The interactions in this parametric study are parallel; that is, the vortex generator is aligned with the rotor centerline. Sound pressure level is plotted as a function of miss distance in Fig. 7a for observers on the retreating side of the rotor where most of the acoustic noise is radiated. The total change in SPL that occurs when the miss distance is increased from 0 to 100% of the chord is 16–17 dB for both of the observers shown.

Hardin and Lamkin[1] suggested that the SPL level decreases as the inverse of the miss distance squared. To determine the relationship between SPL and miss distance, the slope m of the SPL-z/c curve (Fig. 7a) was determined by

$$m = \frac{\mathrm{SPL}_n - \mathrm{SPL}_{n-1}}{10\log_{10}(z/c|_n) - 10\log_{10}(z/c|_{n-1})} \tag{5}$$

and is plotted in Fig. 7b. The slope changes with the location of the observer. When the observer is in the area of high acoustic radiation, found by computationally surveying the sound field, and when the miss distance is less than the core

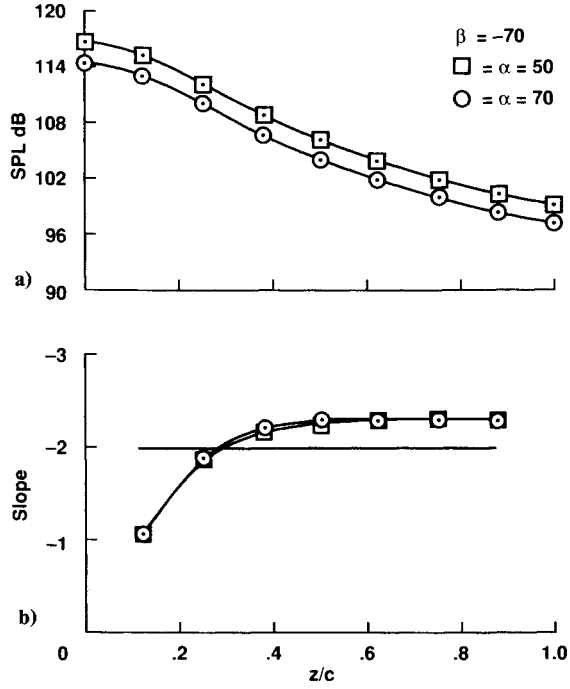

Fig. 7 a) Sound pressure level (SPL) plotted as a function of miss distance z/c for two observer locations and b) slopes of the SPL-z/c curves.

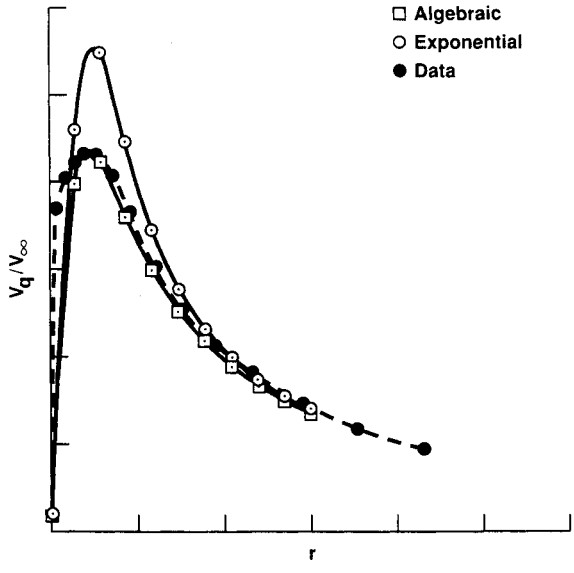

Fig. 8 Comparison of V_q/V_∞ as a function of the radial distance from the vortex center r for the exponential vortex core model, the algebraic vortex core model, and experimental data: vortex core size is $a/C_G = 0.048$ and the vortex strength is $\Gamma/V_\infty C_G = 0.35$.

radius, SPL drops off approximately as the inverse of the miss distance. When the miss distance is greater than the core radius, the tendency is for SPL to drop off approximately as the inverse of the miss distance squared. There is a transition region where the miss distance is approximately the same as the core radius.

Core Size

Another approach to reducing BVI noise is to increase the size of the vortex core. To address the core size issue in this parametric study, the core radius was varied from $0.05c$ to $0.50c$ whereas all other parameters were held constant: $\Gamma = -0.17a_0c$, $\mu = 0.197$, and $M_h = 0.713$. Also, to determine how sensitive this analysis is to the vortex core model, two vortex core models were used. One was the exponential model of Eq. (3), the other was an algebraic vortex model derived by Sculley[20]

$$V_q = \frac{\Gamma}{2\pi r}\left(\frac{r^2}{r^2+a^2}\right) \tag{6}$$

Here r, a, and Γ are defined as in Eq. (3). In Fig. 8, the exponential vortex core model and the algebraic vortex core model are compared to experimental data. This data, measured by McAlister and Takahashi,[19] is for a vortex shed from a fixed vortex generator similar to the one used in this study. The measurements were made four chord lengths behind the trailing edge of the vortex generator. For the comparisons shown in Fig. 8, $a/C_G = 0.048$ and $\Gamma/V_\infty C_G = 0.35$. The algebraic model compares better to the measured data than the exponential model does. However, either model is suitable for this type of parametric study.

SPL is plotted as a function of core radius in Fig. 9a for two miss distances, $z/c = -0.125c$ and -0.25, using both core models. For these cases, the vortex generator was located such that the interactions were parallel. The slopes of the SPL-a/c curves are plotted in Fig. 9b. The slopes were determined as in Eq. (5) with z/c in the denominator replaced by a/c. The difference in SPL between the two core models is small when the core size is smaller than the miss distance. As the core size increases, the difference in SPL between the two models approaches 2 dB.

The fall-off rate of SPL with core radius is very small when the core radius is smaller than the miss distance z/c. This is because the magnitude of the induced velocity at the blade has dropped from V_{max} at a and approaches $1/r$ at z/c. Also, the fall-off rate of SPL for the exponential model is less than that of the algebraic model for the small core sizes. This is because, as the velocity drops from V_{max}, it approaches $1/r$ more quickly for the exponential model than it does for the algebraic model. As the core radius increases the fall-off rate increases because the induced velocity at the blade decreases [see Eqs. (3) and (6)].

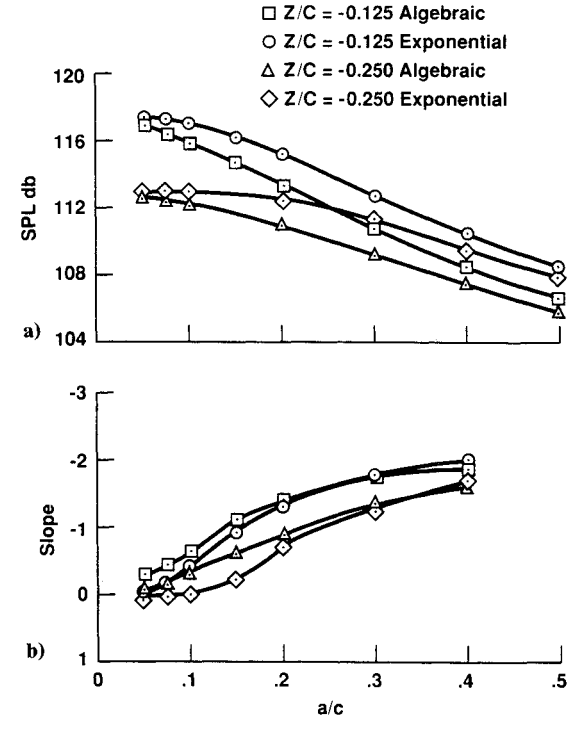

Fig. 9 a) Sound pressure level (SPL) plotted as a function of core radius a/c for both the exponential and algebraic core models and for $z/c = -0.125$ and -0.25 and b) slopes of the SPL-a/c curves.

The fall-off rate of SPL with core radius does approach the inverse of the square of the core radius for the larger core sizes. However, measurements made by McAlister and Takahashi[19] indicate that the core radius is typically $a/c = 0.025$ to 0.050 at seven chords behind the trailing edge of the vortex generator. Dispersion or other tip devices need to increase the core radius to $a/c \geq 0.40$ for this technique to be as effective as increasing the miss distance at reducing BVI noise.

Rotor Speed

The effect of rotor speed on BVI noise is not as simple as the effects of the vortex parameters: strength, core size, and location. A change in rotor speed not only affects the vortex strength, it also affects the rate of blade-vortex interaction and the acoustic radiation through the Doppler factor. For the rotor speed study, core size $a/c = 0.17$ and advance ratio $\mu = 0.197$ are held constant. The freestream velocity V_∞ changes with the rotor rotational speed as prescribed by $V_\infty = \mu\Omega R$. The strength of the vortex produced by the vortex generator is a function of the freestream velocity and must change accordingly. In a realistic BVI environment, the vortex strength is a function of $U = \Omega R\,[(r/R) + \mu \sin \Psi]$. A simplistic view would be to assume that the vortex strength is not a function of Ψ, the rotor azimuth angle, and depends only on $U_s = \Omega R\,[(r/R) \pm \mu]$. If this simplification is accepted and the advance ratio is held constant, the SPLs can be plotted as a function of the hover-tip Mach number $M_h = \Omega R/a_0$. As stated earlier, the vortex strength used in this parametric study is based on measurements made in Ref. 19. The nondimensional vortex strength is $\hat{\Gamma} = \Gamma/V_\infty C_G = 0.406$. For use in FPR, this nondimensional parameter was converted to $\Gamma' = \hat{\Gamma} V_\infty C_G/a_0 c$ or $0.406\mu M_h C_G/c$. The last expression clarifies the dependence of the vortex strength on the hover-tip Mach number. In Fig. 10a, the SPLs are plotted as a function of M_h for two miss distances $z/c = -0.25$ and -0.50 at an observer located 70 deg to the left of the centerline and 40 deg below the tip-path plane. The slopes of the SPL-M_h curves for the two miss distances are shown in Fig. 10b. These slopes are calculated using Eq. (5) with z/c replaced with M_h. The slopes vary slightly with miss distance but are fairly constant over the range of M_h included in this study. These results indicate that SPL increases approximately as M_h^8.

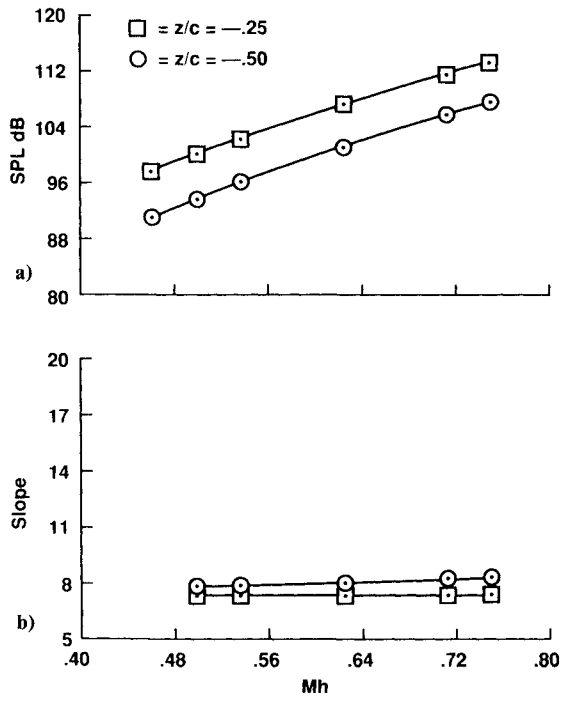

Fig. 10 a) Sound pressure level (SPL) plotted as a function of hover-tip Mach number M_h for $z/c = -0.25$ and -0.50 and b) slopes of the SPL-M_h curves.

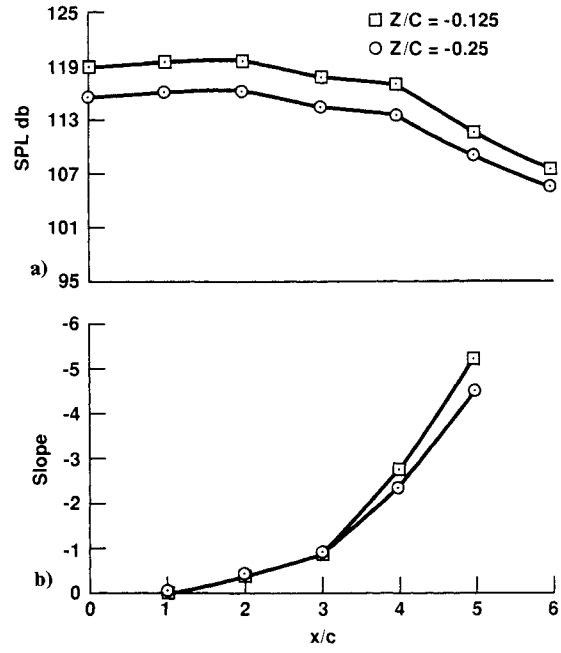

Fig. 11 a) Sound pressure level (SPL) plotted as a function of obliqueness of interaction x/c for $z/c = -0.125$ and -0.25 and b) slopes of the SPL-x/c curves.

Dimensional analysis performed by Lowson[21] indicates that the SPL increases as M_h^6 for dipole type sources and as M_h^8 for quadrapole type sources.[21] Since the calculations indicate that SPL increases as M_h^8, this could imply that additional sound is generated by sources that have been accelerated. This would support the view of Hardin and Lamkin[1] that the acceleration of the vortex results in sound being radiated.

Obliqueness

In descending flight, most interactions of the rotor with a vortex are not completely parallel. Therefore, a study of the obliqueness of interaction is included. For this study, the vortex strength $\Gamma = -0.171 a_\infty c$, the advance ratio $\mu = 0.197$, the hover-tip Mach number $M_h = 0.713$, and the core size $a = 0.17c$ were held constant. The obliqueness of the interaction is determined by the placement of the vortex generator. When the generator is to the right or left of the rotor centerline, the interaction will be oblique. Six cases have been included in this study with x/c ranging from 0.0 to -6.0. These cases are all to the right of the centerline. For these oblique cases, the force terms in the FW-H equation are modeled with 10 spanwise source locations distributed over the outer 50% of the span. This was done to alleviate any concern that the BVI events, which sweep spanwise across the blade, would not be captured by using only five radial stations.

The azimuthal location of the interaction governs the speed of the rotor at the time of interaction and affects the directionality and amplitude of the radiated noise. This makes it difficult to compare the SPLs of the parallel case and the oblique cases at one observer location. Therefore, in Fig. 11a, SPL has been plotted as a function of obliqueness x/c for two miss distances at the observer location of maximum radiation for each case. As stated earlier, the location of maximum radiation is found by computationally surveying the sound field. The slopes of the SPL-x/c curves are plotted in Fig. 11b and show that the fall-off rate increases with an increase in $|x/c|$.

Conclusions

A parametric study has been performed for an isolated blade-vortex interaction using the output from FPR to provide RAPP with the sectional aerodynamic coefficients. Variations

in SPL with miss distance, core size, hover-tip Mach number, and obliqueness of interaction have been presented. For parallel interactions, SPL decreases approximately as the inverse of the miss distance squared in the areas of high acoustic radiation when the miss distance is greater than the vortex core radius. The SPL fall-off rate with core size is very small when the core radius is less than the miss distance. This is obvious for both viscous core models used. When it is assumed that the vortex strength is not a function of the rotor azimuth angle, the calculations indicate that SPL increases approximately as M_h^8. Finally, the fall-off rate of SPL increases with obliqueness of interaction and is only slightly affected by miss distance.

Future work in the prediction of rotor-blade surface pressure will be based on advanced algorithms specifically designed for vortex capturing and there will be no need to model the vortex or prescribe its strength, core size, and location. This will provide a better understanding of the physics involved in blade-vortex interactions and lead to reduced noise generation.

Acknowledgments

This author would like to thank Roger Strawn of the U.S. Army Aeroflightdynamics Directorate for his help in executing FPR and interpreting the results. I would like to thank the research staff of the Fluid Mechanics Division of the Aeroflightdynamics Directorate for the informative discussions, helpful comments, suggestions, and encouragement.

References

[1]Hardin, J. C., and Lamkin, S. L., "Concepts for Reduction of Blade/Vortex Interaction Noise," *Journal of Aircraft,* Vol. 24, No. 2, 1987, pp. 120–125; see also AIAA Paper 86-1855, July 1986.

[2]Splettstoesser, W. R., Lehmann, and Van Der Wall, B., "Initial Results of a Model Rotor Higher Harmonic Control (HHC) Wind Tunnel Experiment on BVI Impulsive Noise Reduction," *Proceedings of the Fifteenth European Rotorcraft Forum*, National Aerospace Laboratories, Amsterdam, The Netherlands, Paper 1, Sept. 1989.

[3]Brooks, T. F., Booth, E. R. Jr., et. al., "HHC Study in the DNW to Reduce BVI Noise—An Analysis," *Proceedings of the AHS-RAeS International Technical Specialists Meeting Rotorcraft Acoustics and Rotor Fluid Dynamics* (Valley Forge, PA), Oct. 1991.

[4]Hoad, D. R., "Evaluation of Helicopter Noise Due to Blade-Vortex Interaction for Five Tip Configurations," NASA TP 1608, Dec. 1979.

[5]Ballard, J., Orloff, K., and Luebs, A., "Effect of Tip Planform on Blade Loading Characteristics for a Two-Bladed Rotor in Hover," NASA TM 78615, Nov. 1979.

[6]Widnall, S., and Wolf, T., "Effect of Tip Vortex Structure on Helicopter Noise Due to Blade-Vortex Interaction," *Journal of Aircraft,* Vol. 17, No. 10, 1980, pp. 705–711.

[7]Strawn, R. C., and Caradonna, F. X., "Conservative Full-Potential Model for Unsteady Transonic Rotor Flows," *AIAA Journal,* Vol. 25, No. 2, 1987, pp. 193–198; see also AIAA Paper 86-0079, Jan. 1986.

[8]Gallman, J. M., "The Validation and Application of a Rotor Acoustic Prediction Computer Program," *Army Science Conference Proceedings,* Vol. II, June 1990, pp. 1–15.

[9]Tadghighi, H., Hassan, A. A., and Charles, B. D., "Prediction of Blade-Vortex Interaction Noise Using Airloads Generated by a Finite-Difference Technique," *Proceedings of the 46th Annual Forum of the American Helicopter Society* (Washington, DC), May 1990, Vol. I, pp. 367–378.

[10]Hassan, A. A., and Charles, B. D., "Simulation of Realistic Rotor Blade-Vortex Interactions Using a Finite-Difference Technique," *Journal of the American Helicopter Society,* Vol. 36, No. 3, 1991, pp. 71–83.

[11]Caradonna, F. X., Lautenschlager, J. L., and Silva, M. J., "An Experimental Study of Rotor-Vortex Interactions," AIAA Paper 88-0045, Jan. 1988.

[12]Caradonna, F. X., and Strawn, R. C., "An Experimental and Computational Study of Rotor-Vortex Interaction," *Vertica,* Vol. 12, No. 4, 1988, pp. 314–327.

[13]Bridgeman, J. O., Steger, J. L., and Caradonna, F. X., "A Conservative Finite-Difference Algorithm for the Unsteady Transonic Potential Equation in Generalized Coordinates," AIAA Paper 82-1388, Aug. 1982.

[14]Strawn, R., and Tung, C., "The Prediction of Transonic Loading on Advancing Helicopter Rotors," NASA TM 88238, US AVSCOM TM 886-A-1, April 1986.

[15]Farassat, F., "Theory of Noise Generation From Moving Bodies with an Application to Helicopter Rotors," NASA TR R-452, Dec. 1965.

[16]Wells, V. L., "Analysis of the Acoustic Planform Method for Rotor Noise Prediction," *AIAA Journal,* Vol. 26, No. 5, 1988, pp. 522–523.

[17]Zinner, R. A., and Boxwell, D. A., "Review and Analysis of the DNW/Model 360 Rotor Acoustic Data Base," *Proceedings of the Fifteenth European Rotorcraft Forum*, National Aerospace Laboratories, Amsterdam, The Netherlands, Paper 4, Sept. 1989.

[18]Boxwell, D. A., Schmitz, F. H., Splettstoesser, W. R., and Schultz, K. J., "Helicopter Model Rotor-Blade Vortex Interaction Impulsive Noise: Scalability and Parametric Variations," *Journal of the American Helicopter Society,* Vol. 32, No. 1, 1987, pp. 3–12.

[19]McAlister, K. W., and Takahashi, R. K., "NACA 0015 Wing Pressure and Trailing Vortex Measurements," NASA TP 3151, USAAVSCOM TR-91-A-003, Aug. 1991.

[20]Sculley, M. P., "Computation of Helicopter Rotor Wake Geometry and Its Influence on Rotor Harmonic Loads," Massachusetts Inst. of Technology, ASRL TR-178-1, Cambridge, MA, March 1975.

[21]Lowson, M. V., "Basic Mechanisms of Noise Generated by Helicopters, V/STOL Aircraft and Ground Effect Machines," *Journal of Sound and Vibration,* Vol. 3, No. 3, 1966, pp. 454–466.